

Long Baroclinic Rossby Waves Identified in the Tropical Atlantic from ARGO Floats

Peter C Chu, Leonid Ivanov Oleg Melnichenko
Naval Postgraduate School
Monterey, CA 93943

Neil C. Wells
Southampton Oceanographic Center, UK

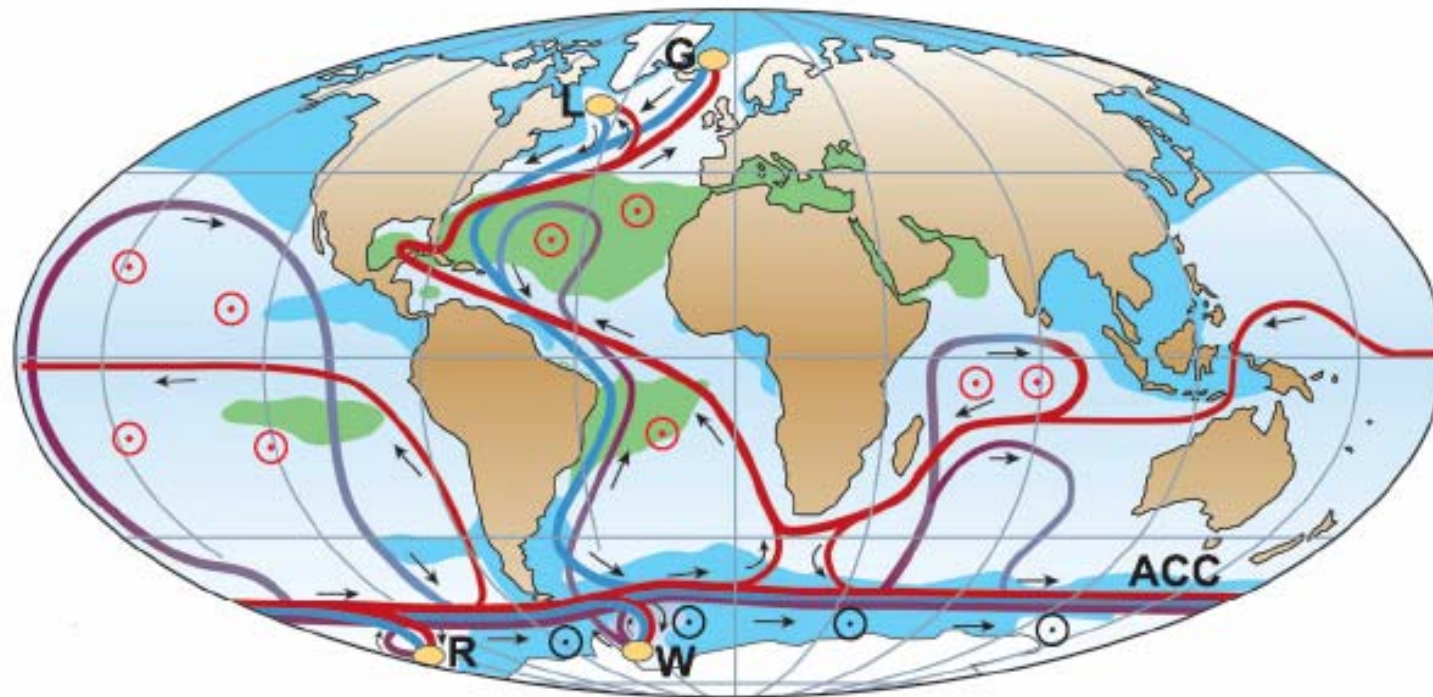
pcchu@nps.edu

<http://www.oc.nps.navy.mil/~chu>

Important Element in Climate System

Meridional Overturning Circulation (MOC)

(Rahmstorf 2006)



- Surface flow
- Deep flow
- Bottom flow
- Deep Water Formation

- ⊙ Wind-driven upwelling
- ⊗ Mixing-driven upwelling
- Salinity > 36 ‰
- Salinity < 34 ‰

- L Labrador Sea
- G Greenland Sea
- W Weddell Sea
- R Ross Sea

Mid-Depth (1000 m) Circulation →

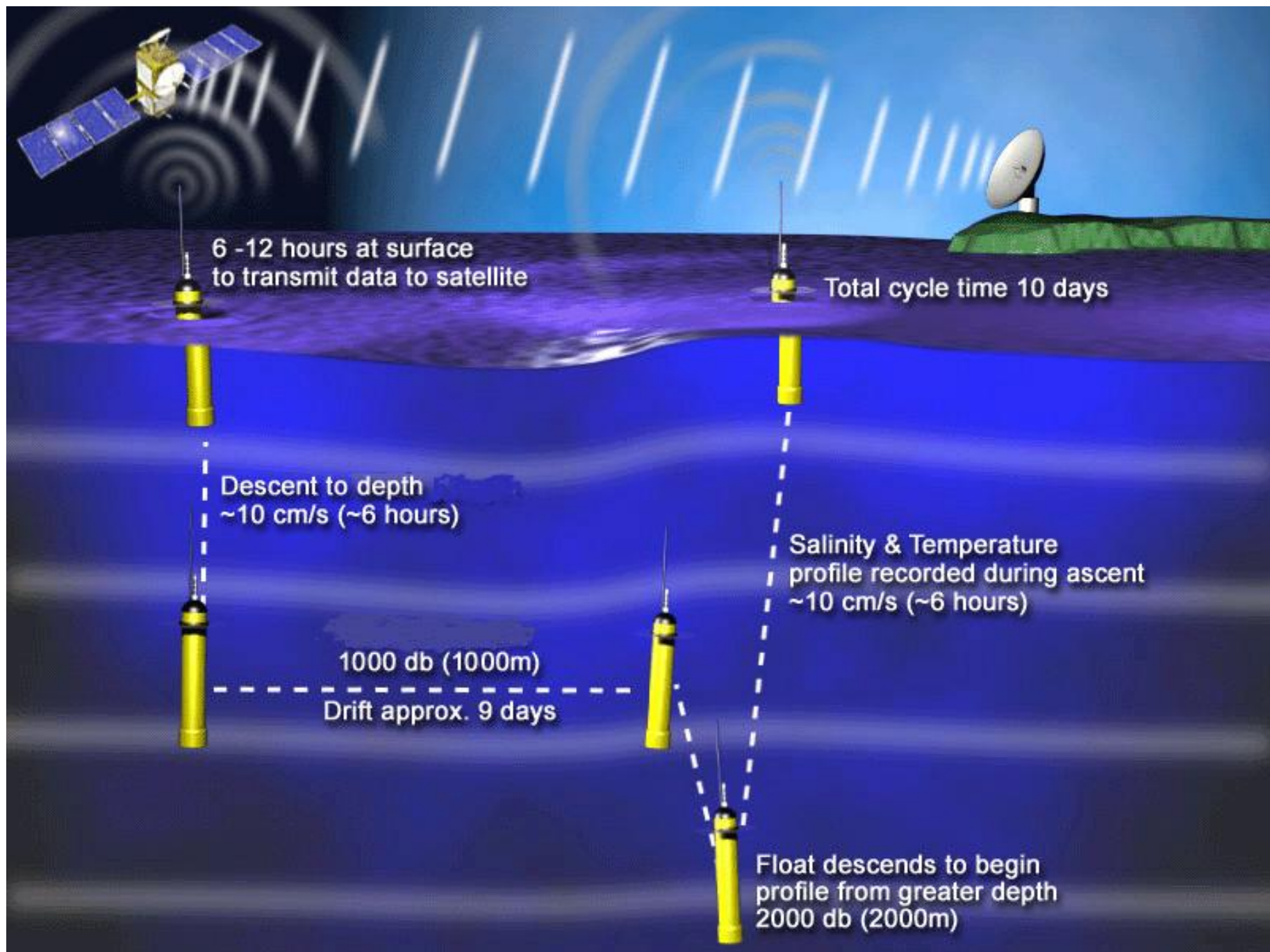
MOC Variation →

Heat Transport Variation →

Climate Change

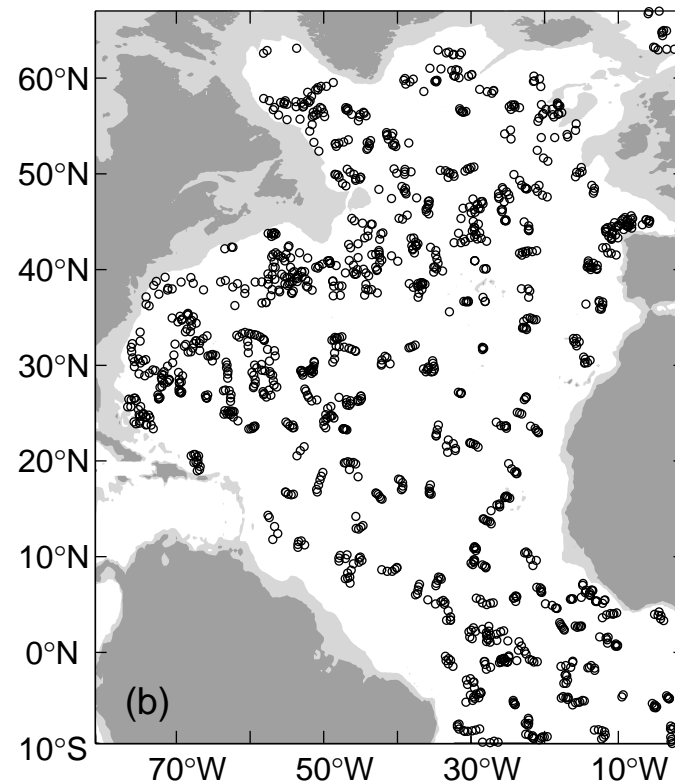
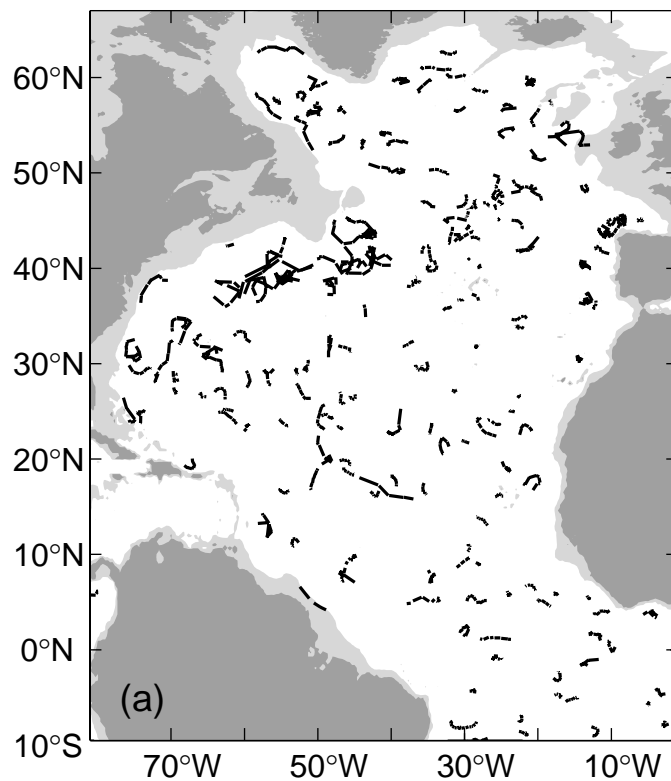
- Q1: Are mid-depth (~1000 m) ocean circulations steady?
- Q2: If not what mechanisms cause the change?

A: Rossby wave propagation



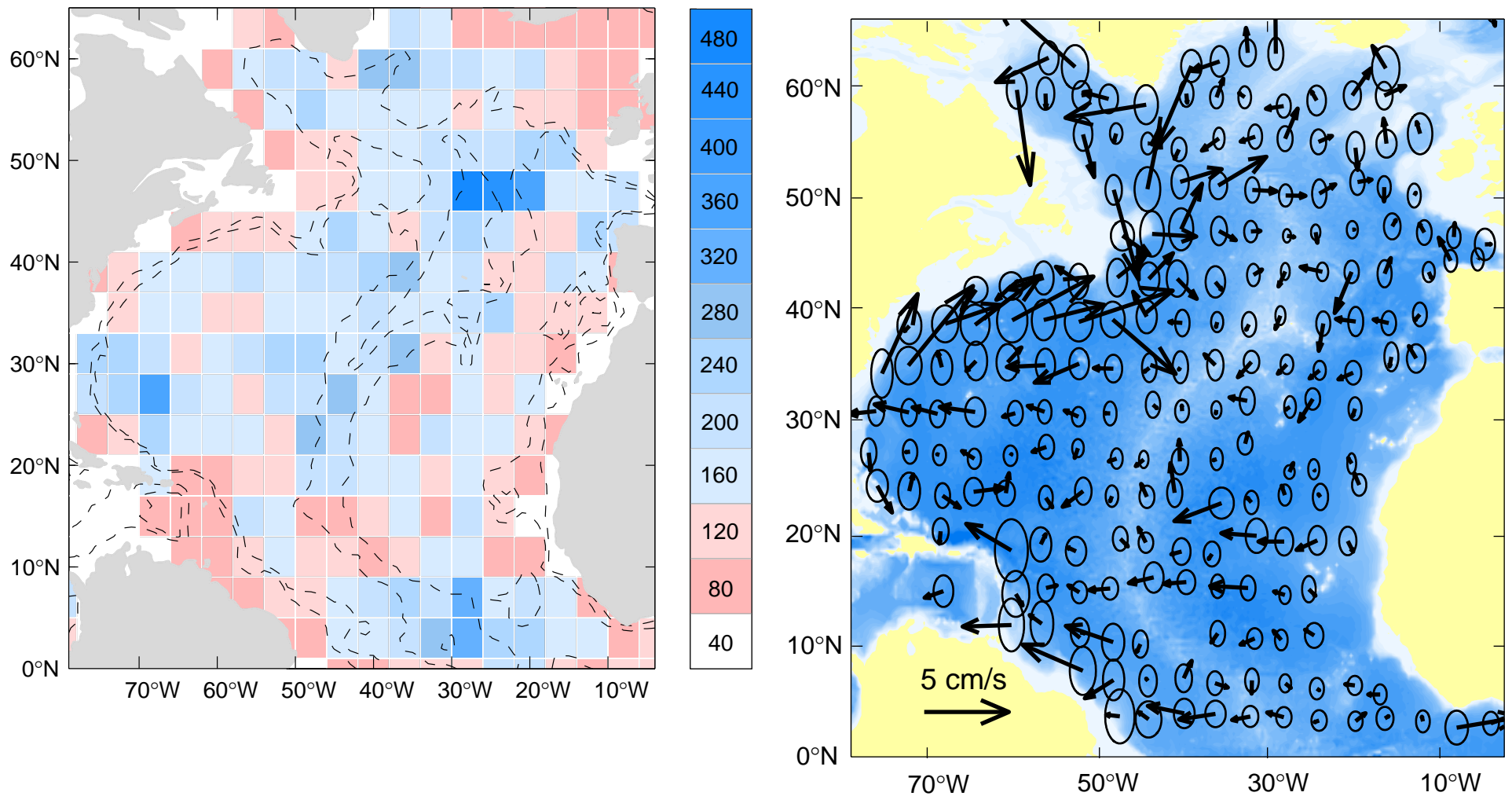
October-November 2004 ARGO

(a) float tracks, and (b) float positions where temperature profiles were measured.



Circulations at 1000 m estimated from the original ARGO float tracks (bin method)

April 2004 – April 2005



OSD

Spectral Representation

$$c(\mathbf{x}, z_k, t) = A_0(z_k, t) + \sum_{m=1}^M A_m(z_k, t) \Psi_m(\mathbf{x}, z_k),$$

**Spatial Variability is represented
by the basis functions**

References

- Chu, P.C., L.M. Ivanov, T.P. Korzhova, T.M. Margolina, and O.M. Melnichenko, 2003a: Analysis of sparse and noisy ocean current data using flow decomposition. Part 1: Theory. *Journal of Atmospheric and Oceanic Technology*, 20 (4), 478-491.
- Chu, P.C., L.M. Ivanov, T.P. Korzhova, T.M. Margolina, and O.M. Melnichenko, 2003b: Analysis of sparse and noisy ocean current data using flow decomposition. Part 2: Application to Eulerian and Lagrangian data. *Journal of Atmospheric and Oceanic Technology*, 20 (4), 492-512.
- Chu, P.C., L.M. Ivanov, and T.M. Margolina, 2004: Rotation method for reconstructing process and field from imperfect data. *International Journal of Bifurcation and Chaos*, 14(8), 2991-2997.
- Chu, P.C., L.M. Ivanov, and O.M. Melnichenko, 2005: Fall-winter current reversals on the Texas-Louisiana continental shelf. *Journal of Physical Oceanography*, 35, 902-910
- Chu, P.C., L.M. Ivanov, O.M. Melnichenko, and N.C. Wells, 2007: On long baroclinic Rossby Waves in the tropical North Atlantic observed from profiling floats. *Journal of Geophysical Research – Oceans*, in press.
- These papers can be downloaded from:
- <http://www.oc.nps.navy.mil/~chu>

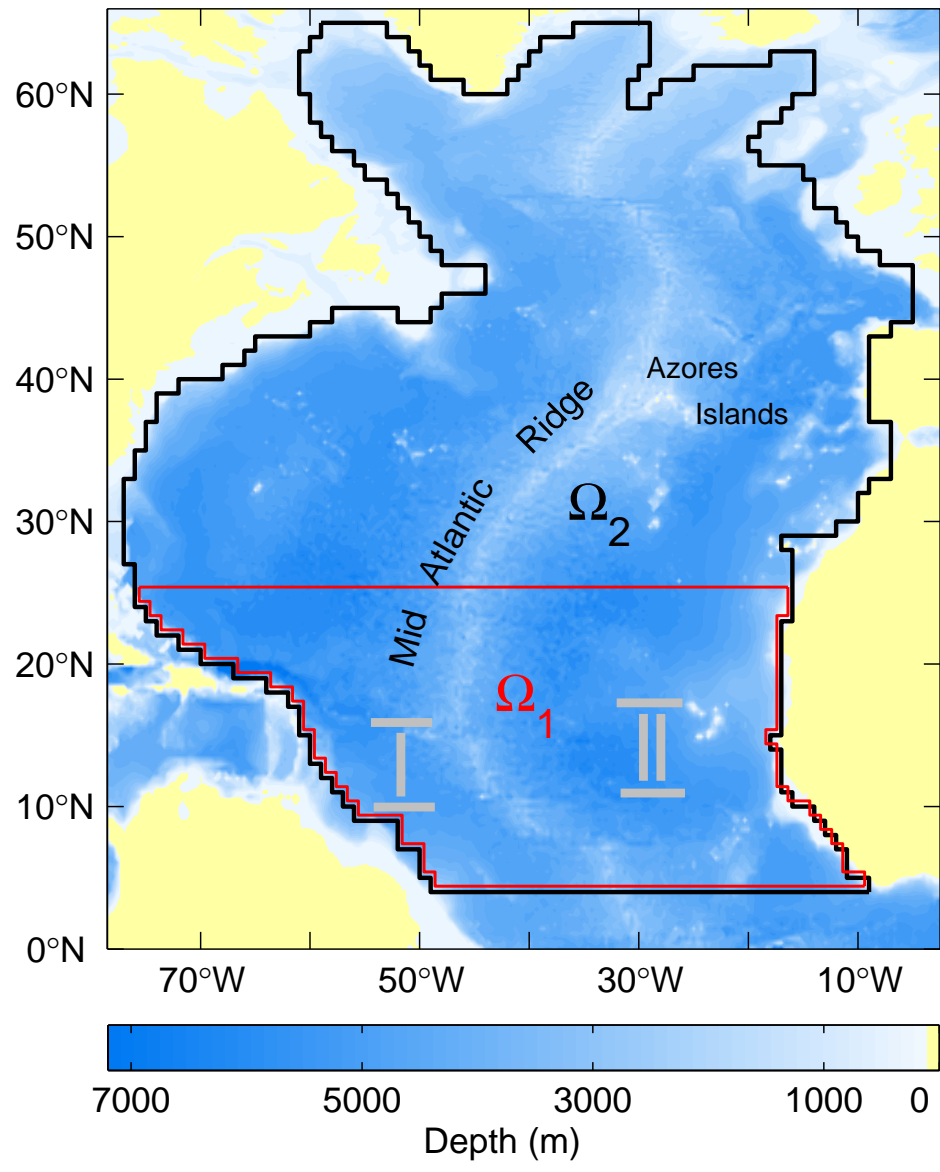
Basis Functions of Laplace Operator (Open Boundaries)

$$\Delta \Psi_k = -\lambda_k \Psi_k,$$

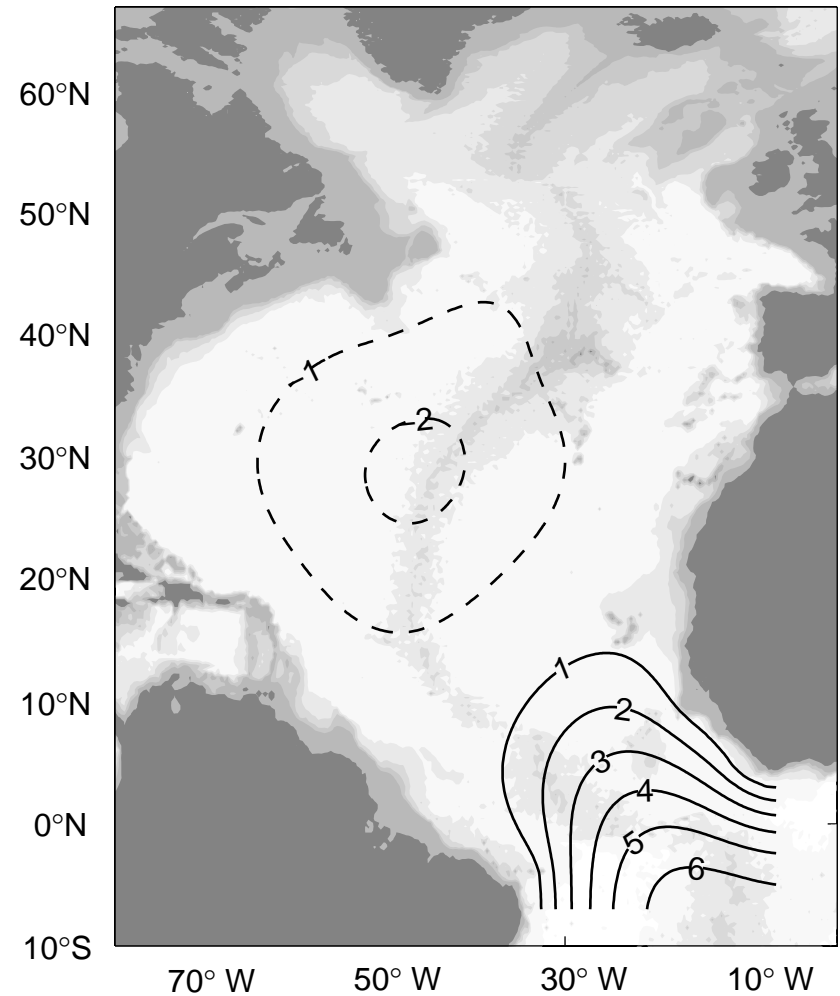
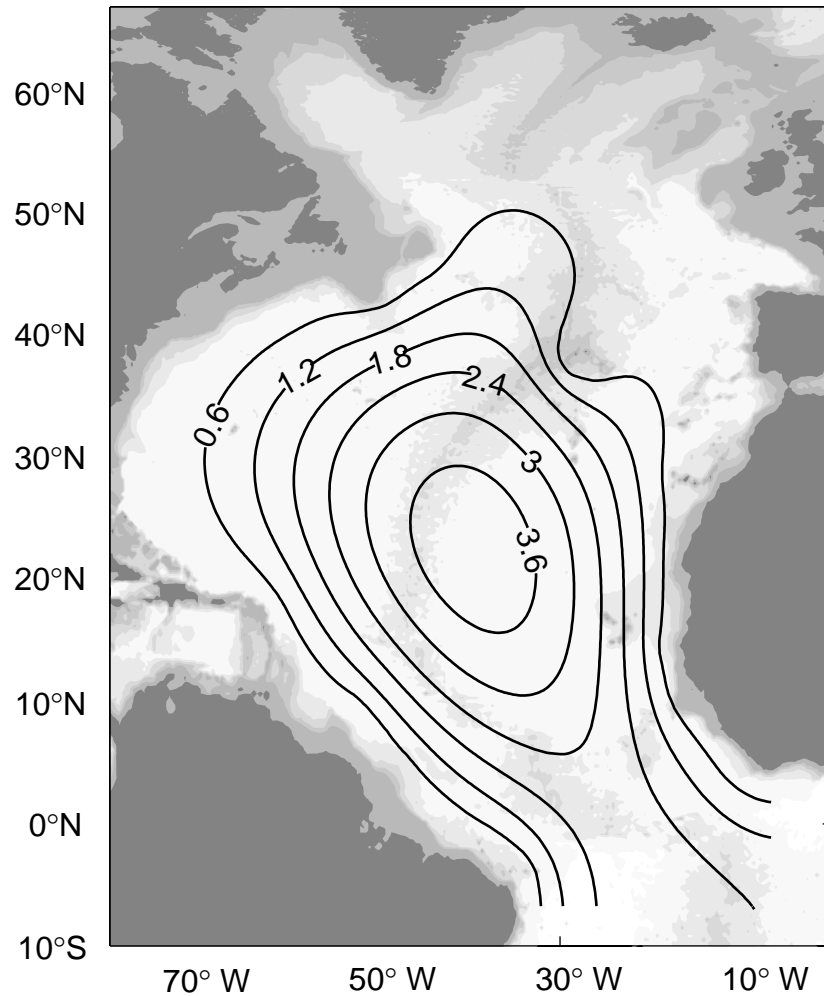
$$\Delta \Phi_m = -\mu_m \Phi_m,$$

$$\Psi_k|_{\Gamma} = 0, \quad \frac{\partial \Phi_m}{\partial n}|_{\Gamma} = 0,$$

$$\left[\frac{\partial \Psi_k}{\partial n} + \kappa(\tau) \Psi_k \right] |_{\Gamma'_1} = 0, \quad \Phi_m|_{\Gamma'_1} = 0,$$



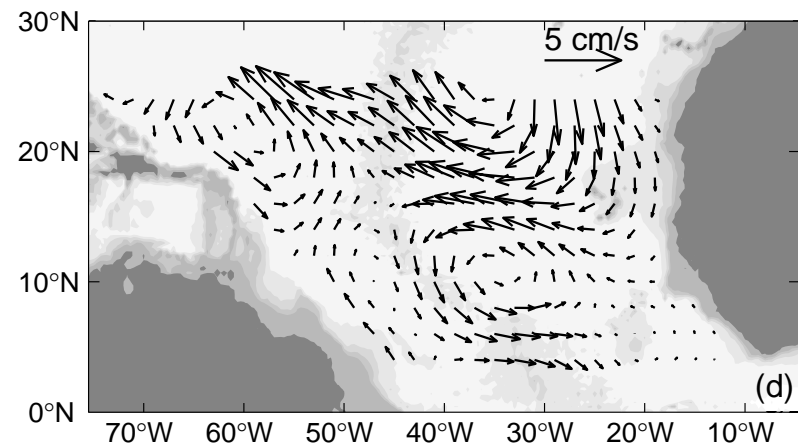
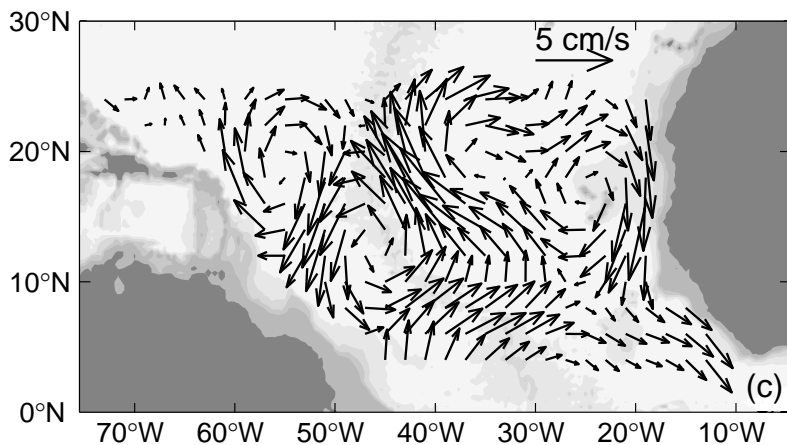
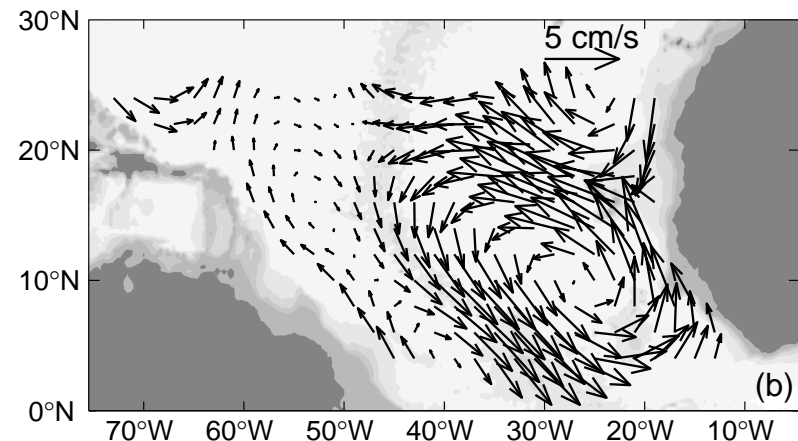
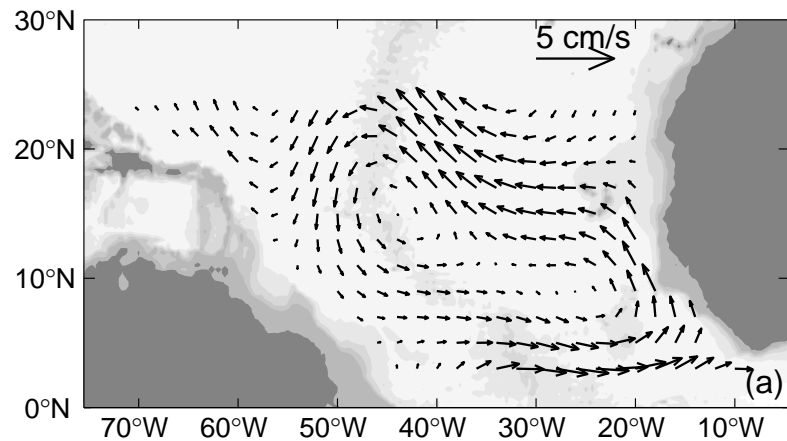
Basis Functions for Streamfunction Mode-1 and Mode-2



Mid-Depth Circulations (1000 m)

(a) Apr 04-Apr 05, (b) Jun-Jul04

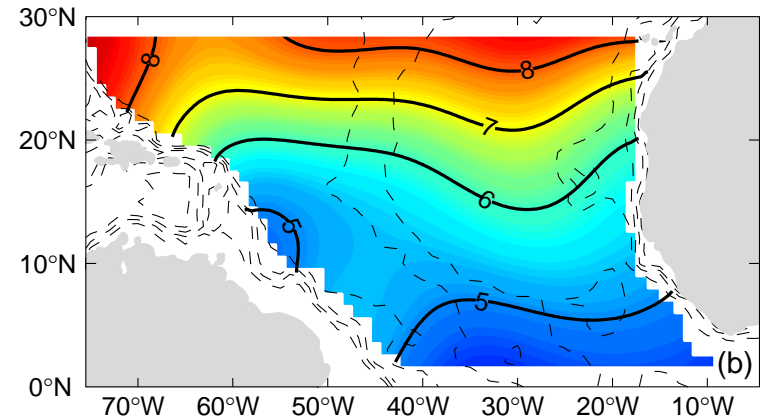
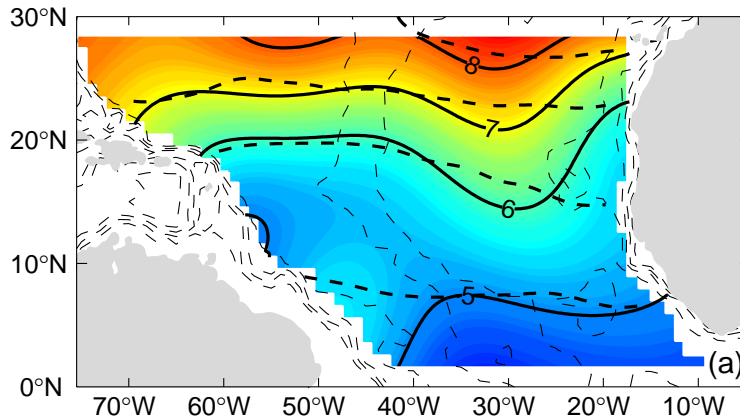
(c) Oct-Nov04, (d) Mar-Apr05



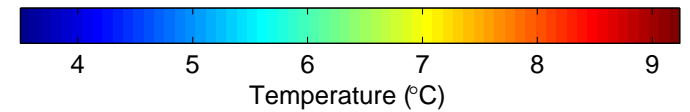
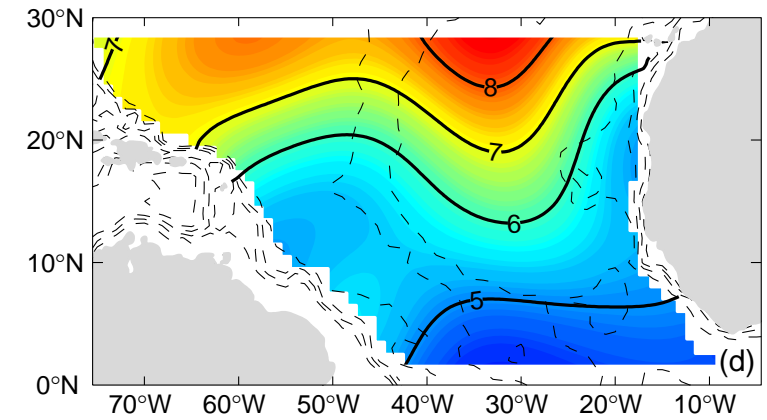
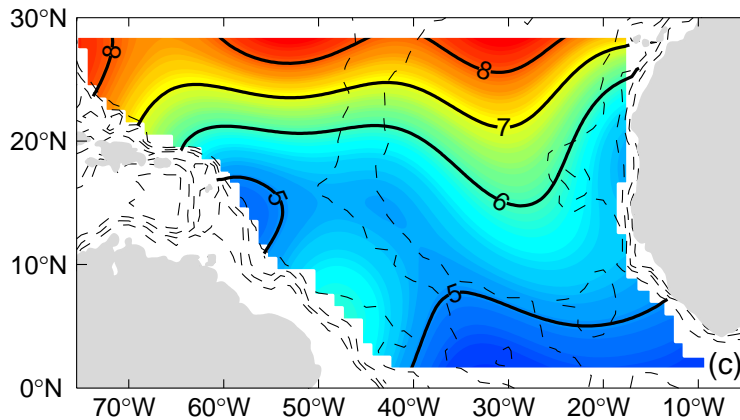
Apr 04 – Apr 05

Jul 04

T
(950 m)



Dashed
Curves
→
WOA



Nov 04

Apr 05

Temporal Decomposition Annual + Semiannual

$$\hat{\psi} \approx \bar{\psi}(\mathbf{x}_{\perp}) + \psi_1(\mathbf{x}_{\perp}, t) + \psi_2(\mathbf{x}_{\perp}, t),$$

$$\psi_1(\mathbf{x}_{\perp}, t) = \sum_{s=1}^2 A_{\omega_1, s} \cos(\omega_1 t + \theta_{\omega_1, s}) Z_s(\mathbf{x}_{\perp}) + \sum_{k=1}^{K_{opt}} B_{\omega_1, k} \cos(\omega_1 t + \vartheta_{\omega_1, k}) \Psi_k(\mathbf{x}_{\perp}),$$

$$\psi_2(\mathbf{x}_{\perp}, t) = \sum_{s=1}^2 A_{\omega_2, s} \cos(\omega_2 t + \theta_{\omega_2, s}) Z_s(\mathbf{x}_{\perp}) + \sum_{k=1}^{K_{opt}} B_{\omega_2, k} \cos(\omega_2 t + \vartheta_{\omega_2, k}) \Psi_k(\mathbf{x}_{\perp}),$$

Temporal Decomposition Annual + Semiannual

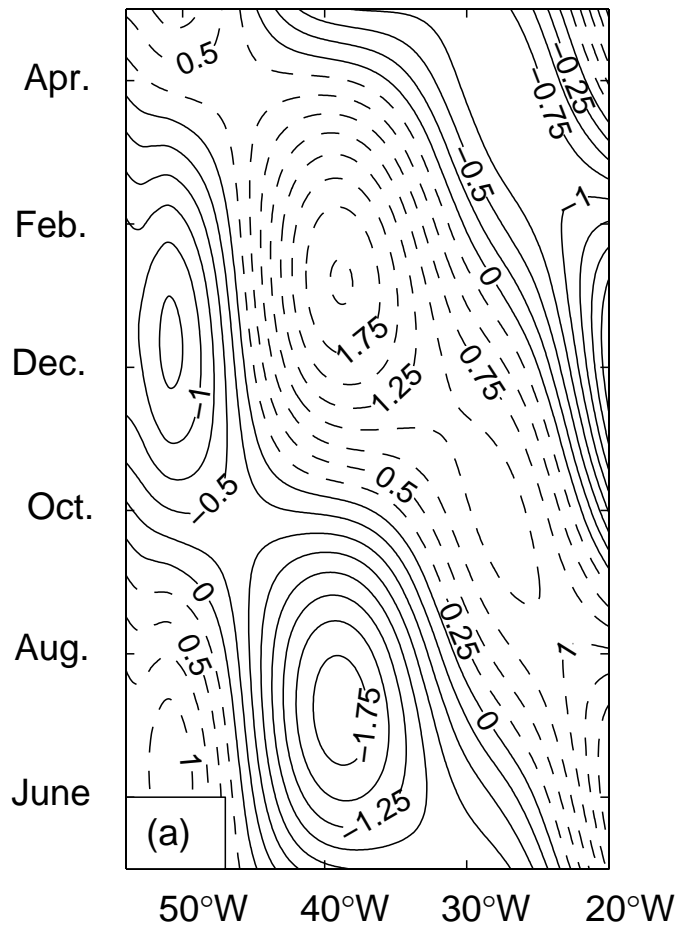
$$\hat{T}(\mathbf{x}_{\perp}, z, t) \approx \bar{T}(\mathbf{x}_{\perp}, z) + T_1(\mathbf{x}_{\perp}, z, t) + T_2(\mathbf{x}_{\perp}, z, t),$$

$$T_1(\mathbf{x}_{\perp}, z, t) = \sum_{m=1}^{M_{opt}} C_{\omega_1, m}(z) \cos[\omega_1 t + \chi_{\omega_1, m}(z)] \Xi_m(\mathbf{x}_{\perp}, z),$$

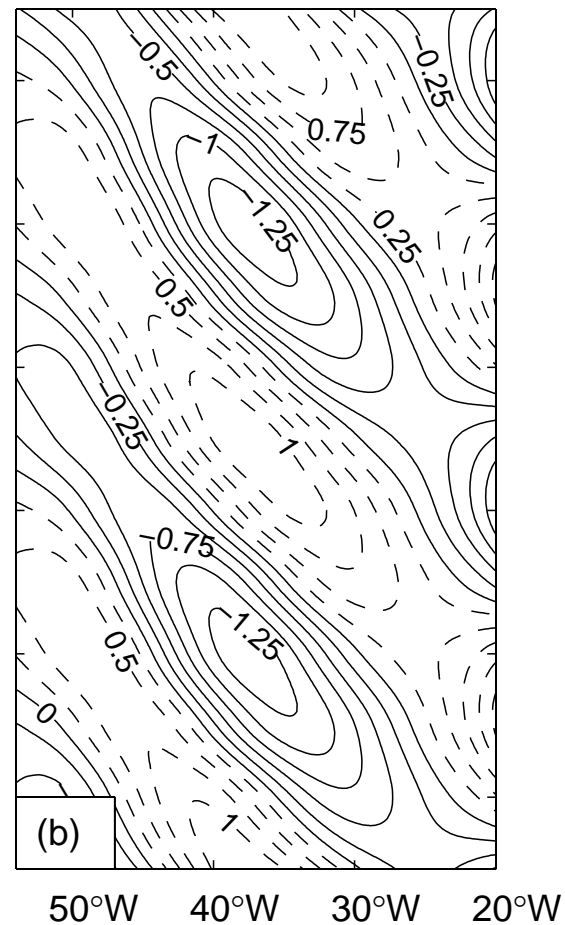
$$T_2(\mathbf{x}_{\perp}, z, t) = \sum_{m=1}^{M_{opt}} C_{\omega_2, m}(z) \cos[\omega_2 t + \chi_{\omega_2, m}(z)] \Xi_m(\mathbf{x}_{\perp}, z),$$

Time-longitude diagrams of meridional velocity along 11°N (cm/s)

Annual



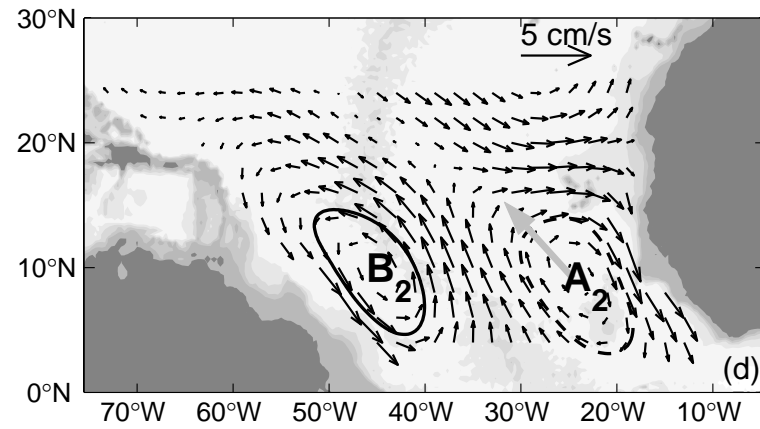
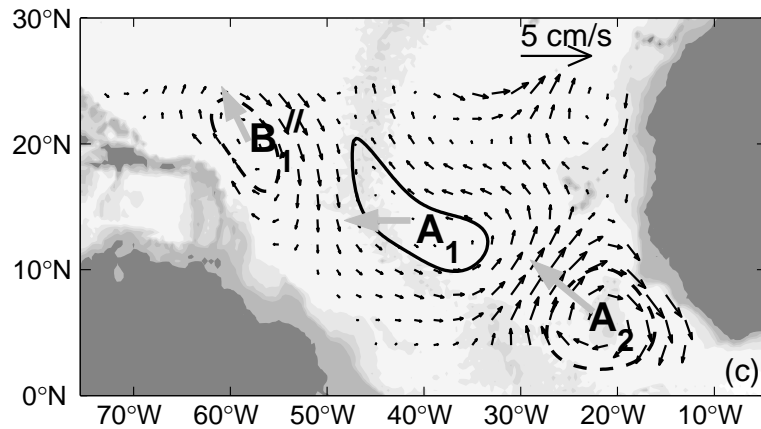
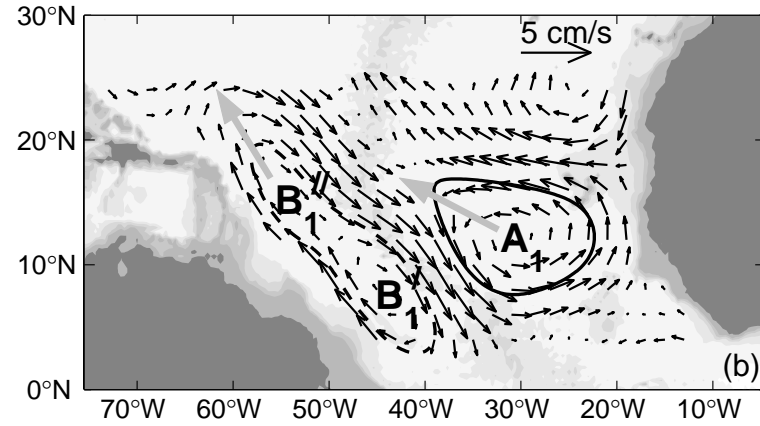
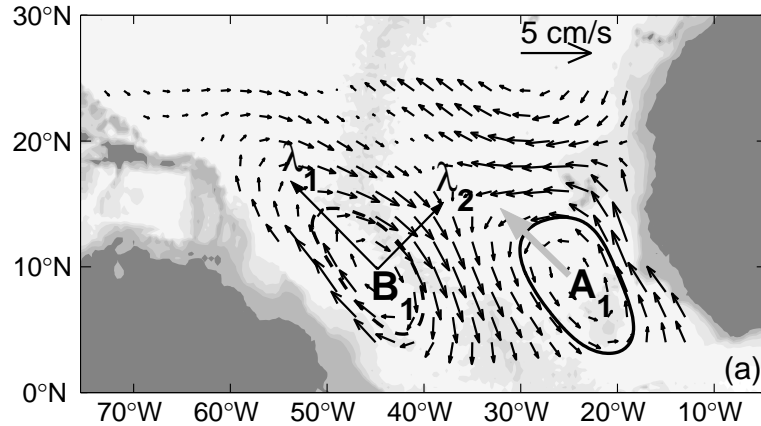
Semi-Annual



Two wave-like signals in Annual currents

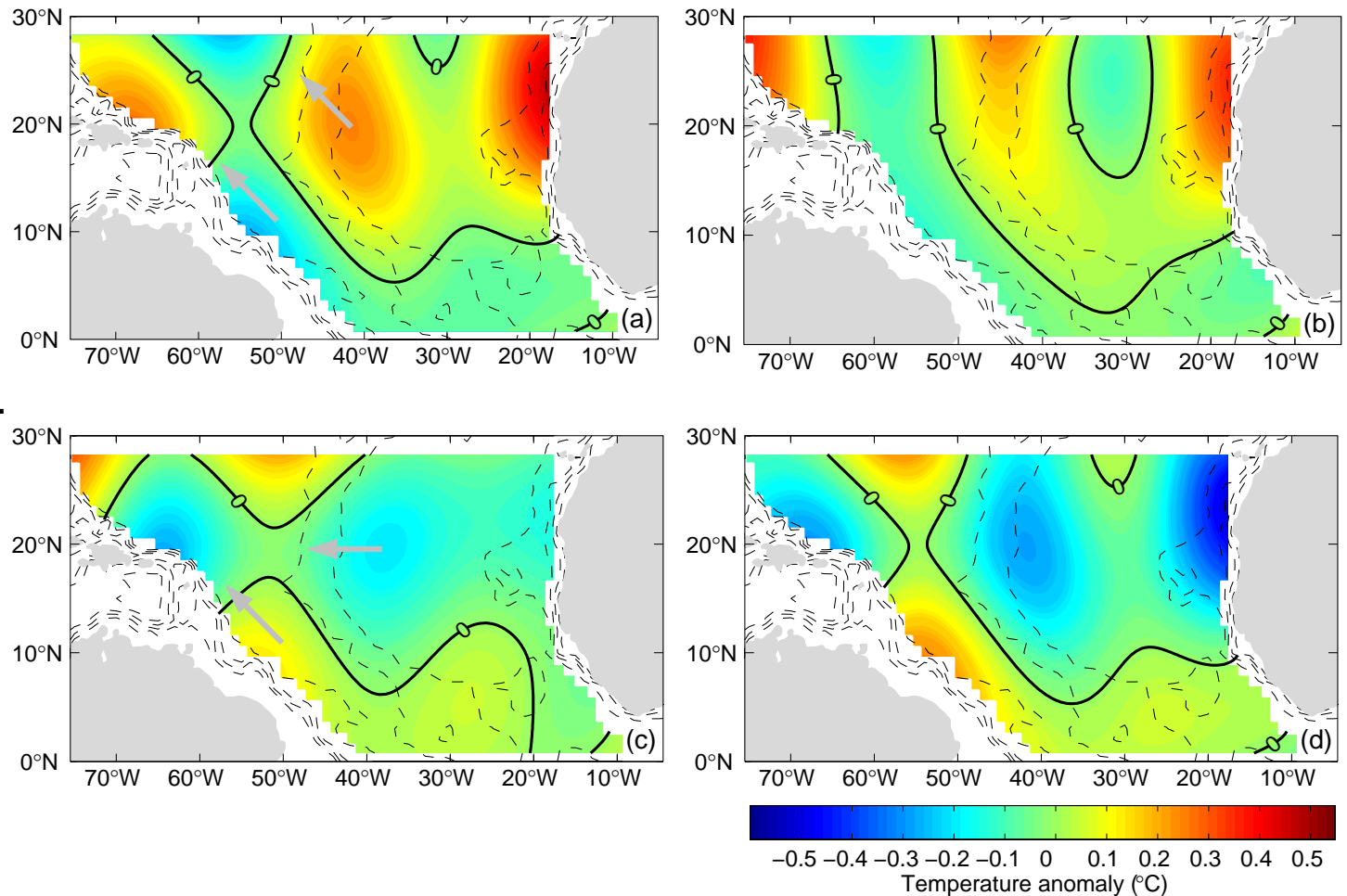
(a) May-Jun 04 (b) Jul-Aug 04

(c) Sep-Oct 04 (d) Nov-Dec 04



Annual monthly temperature anomaly at 950m depth

- (a) Jun 04
- (b) Aug 04
- (c) Oct 04
- (d) Dec 04.

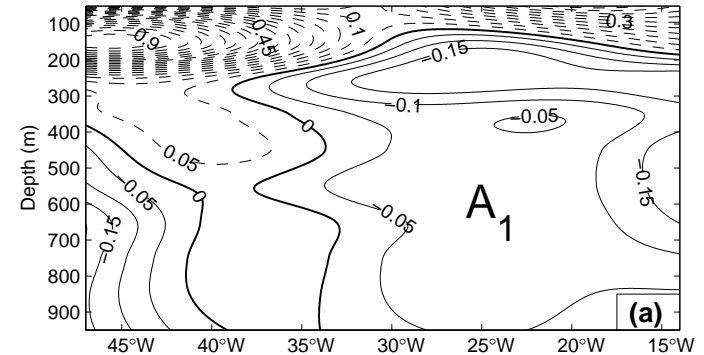


Kinematic characteristics of the annual Rossby wave propagating in the eastern sub-basin

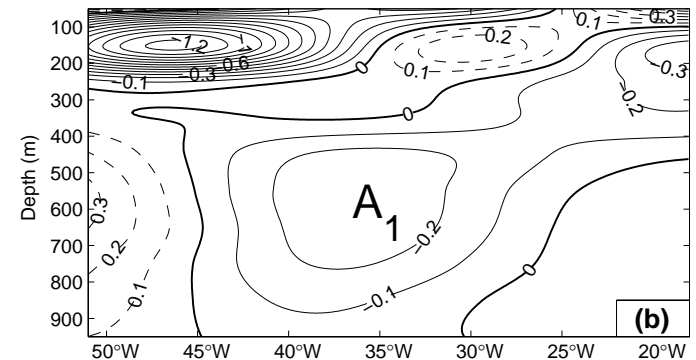
	March, 04 – May, 05 float data			March, 04 – May, 06 float data		
Latitude	c_p (cm/s)	L_1 (km)	L_2 (km)	c_p (cm/s)	L_1 (km)	L_2 (km)
5°N	12	1200	1100	12	1300	900
8°N	16	2500	1400	12	2100	1100
11°N	14	2200	1400	11	1900	1100
13°N	11	2100	1500	10	2300	1500

Zonal cross-sections of the annual component of the temperature anomaly ($^{\circ}\text{C}$)

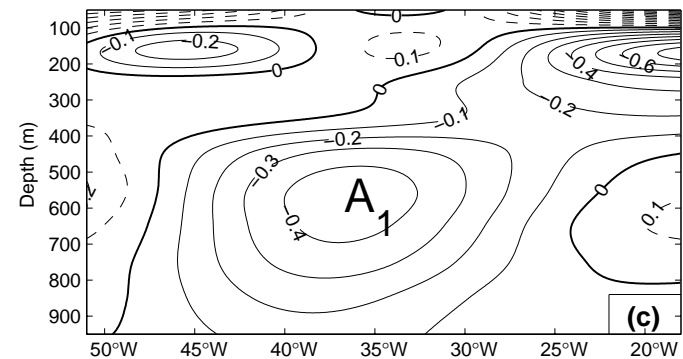
6 $^{\circ}\text{N}$ in Jun 04 \rightarrow



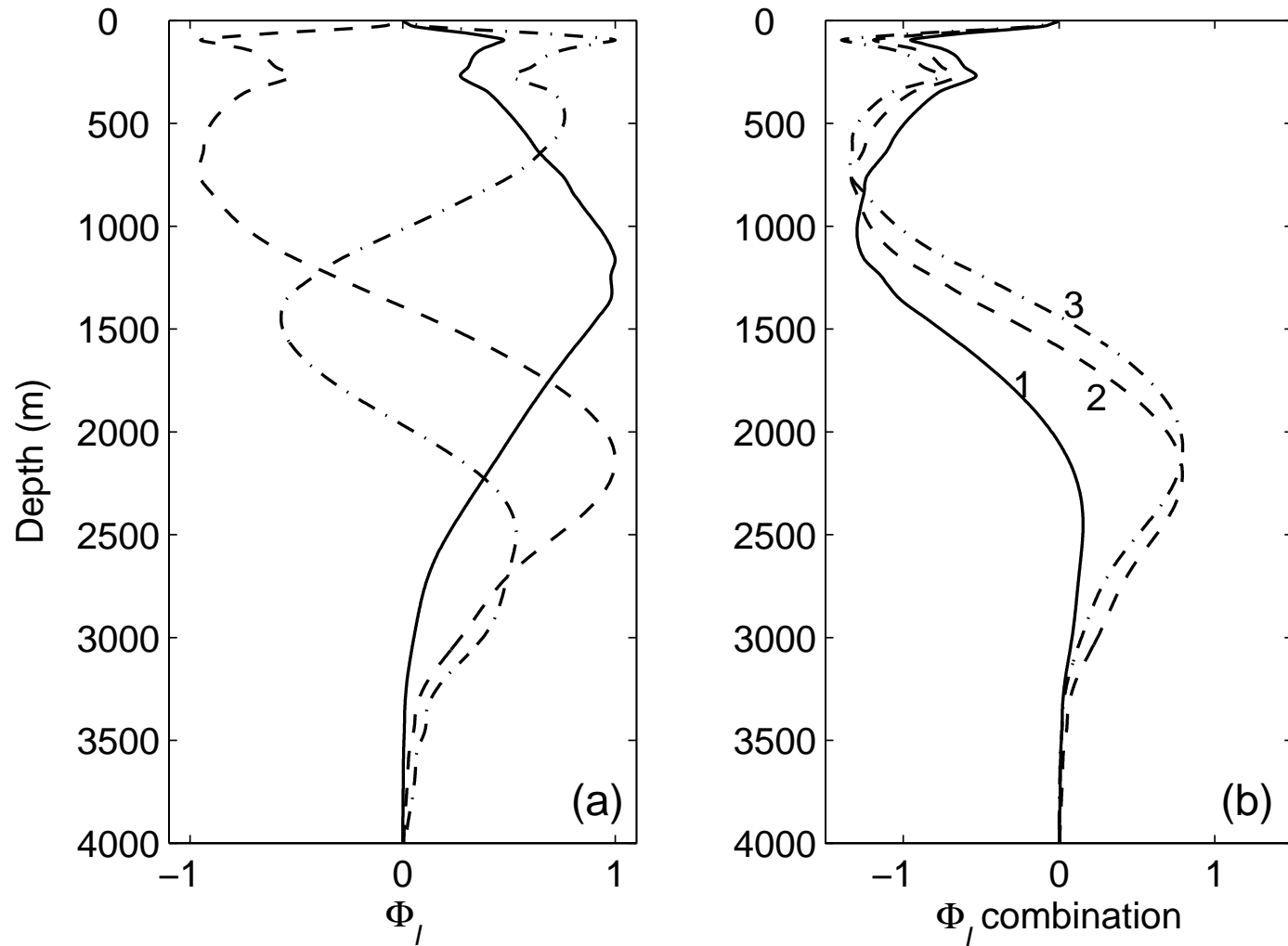
11 $^{\circ}\text{N}$ in Oct, 04 \rightarrow



16 $^{\circ}\text{N}$ in Oct 04 \rightarrow

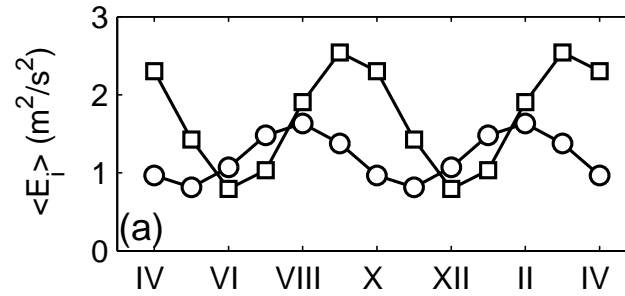


Baroclinic Modes



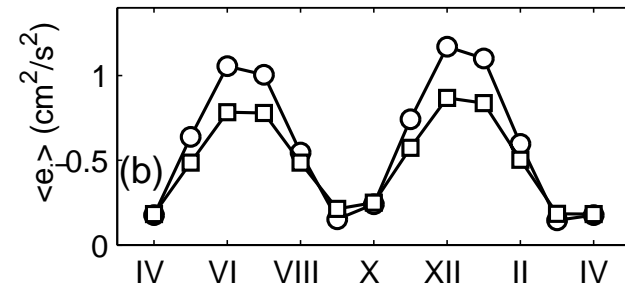
Annual Component in the Western Sub-Basin

Mean wind KE



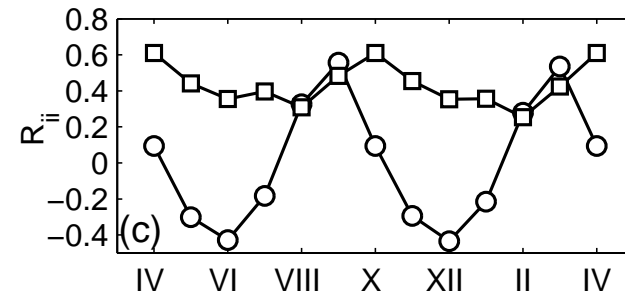
Zonal: circle

Mean KE for mid-depth currents

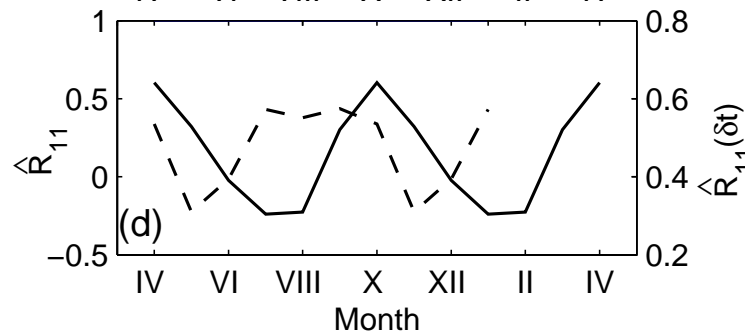


Meridional :
square

Correlation between Winds and currents



Correlation between wind Stress curl and streamfunction
(solid: no-lag, dashed: 3 mon lag)



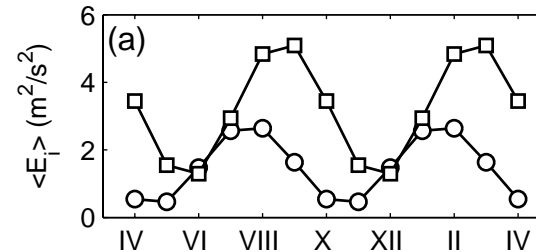
Annual Component in the Eastern Sub-Basin

Mean wind KE

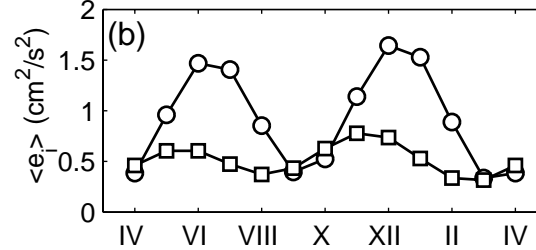
Mean KE for mid-depth currents

Correlation between Winds and currents

Correlation between wind Stress curl and streamfunction
(solid: no-lag, dashed: 3 mon lag)

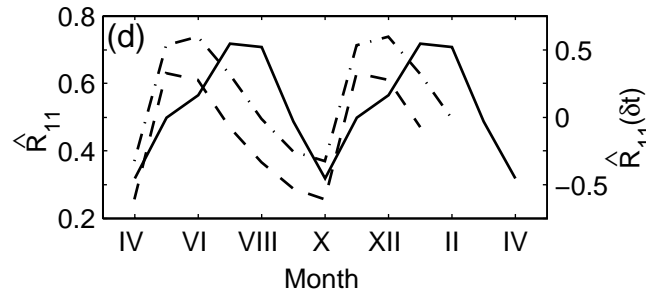
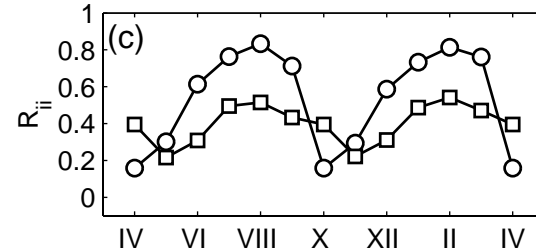


Zonal: circle



Meridional :

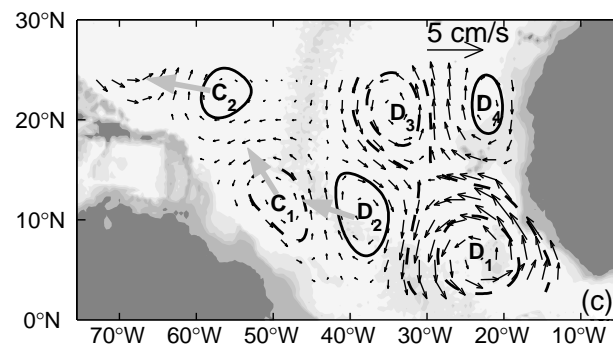
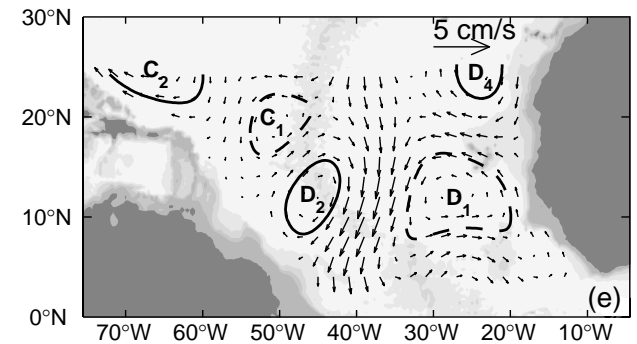
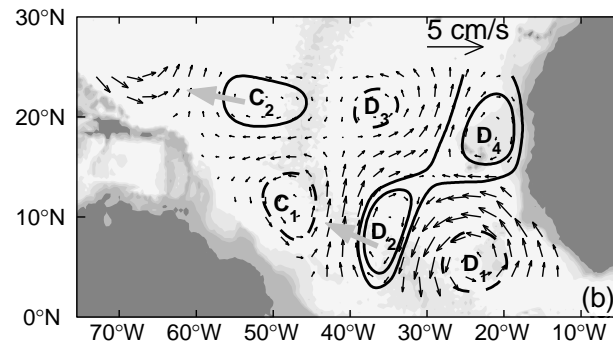
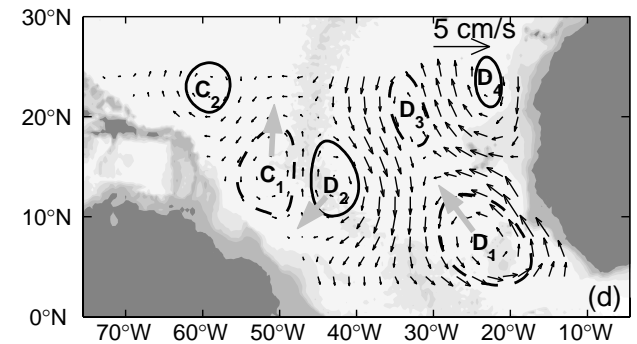
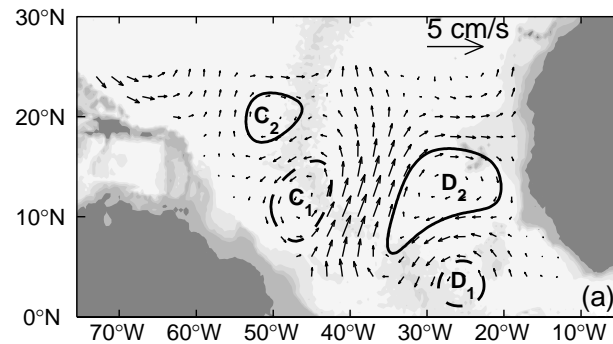
square



Month

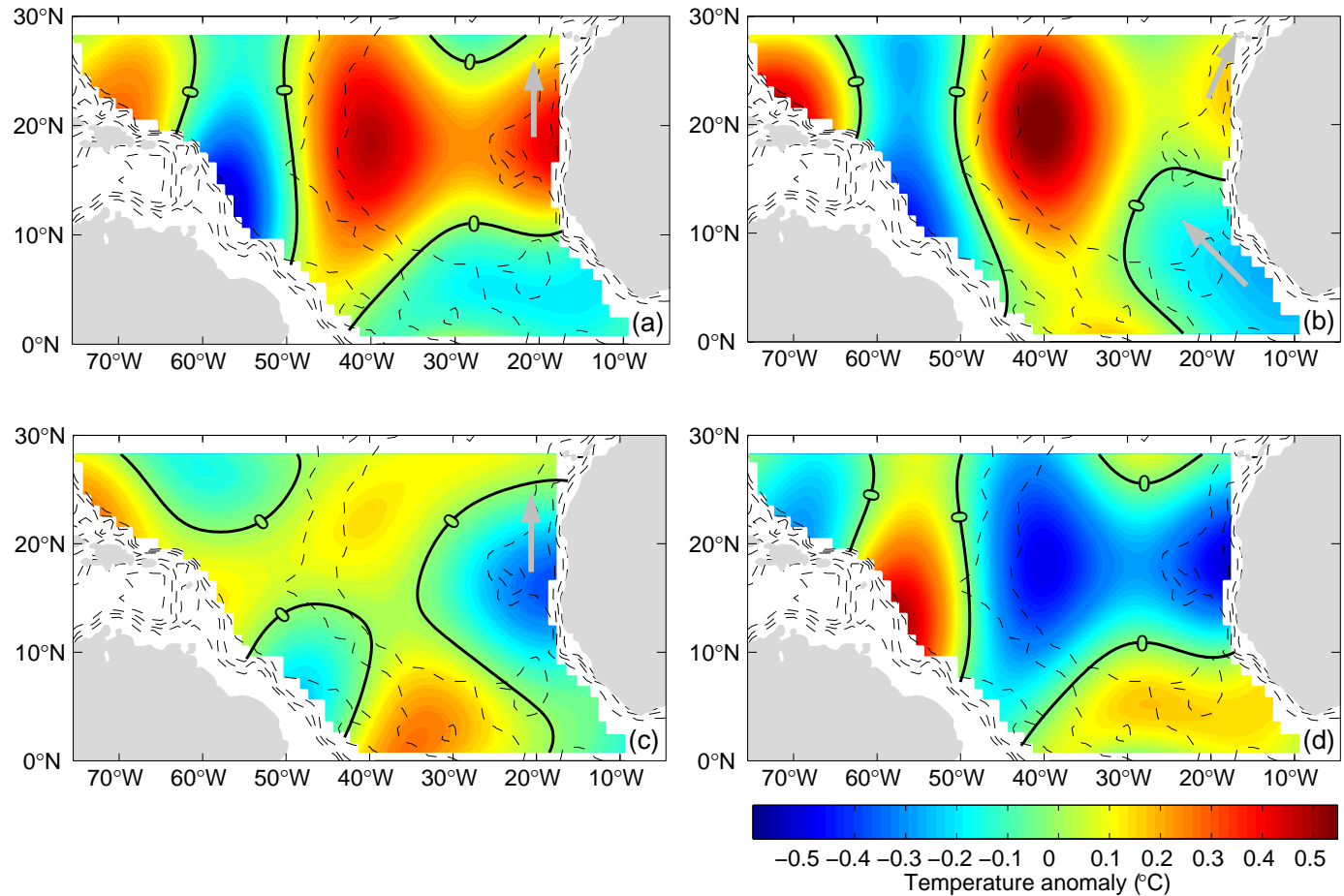
Semi-annual currents at 1000 m depth (2004)

- (a) 5/15**
- (b) 5/30**
- (c) 6/14**
- (d) 6/29**
- (e) 7/13**



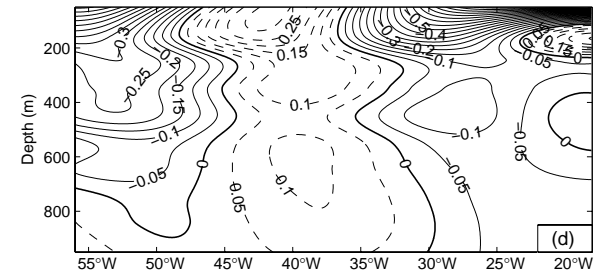
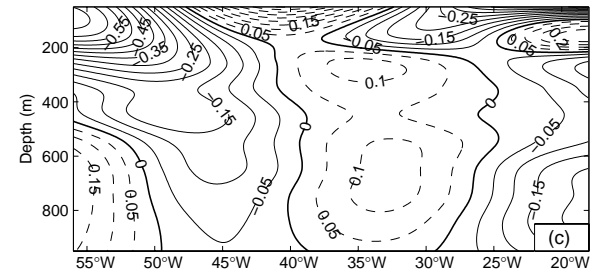
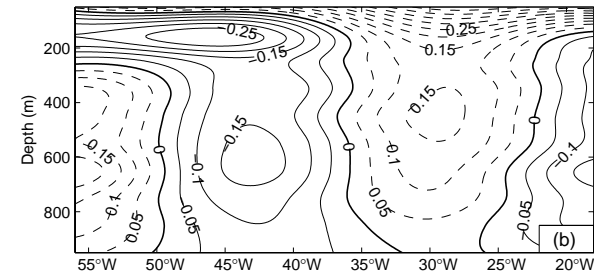
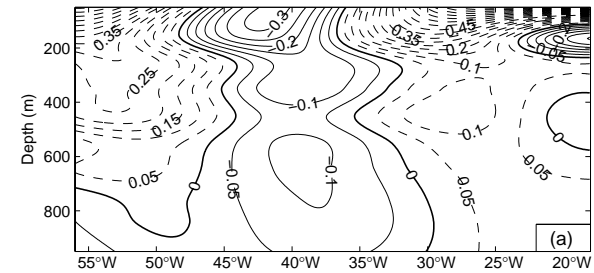
Semi-annual monthly temperature anomaly at 950m depth

- (a) Jun 04
- (b) Aug 04
- (c) Oct 04
- (d) Dec 04.



Semi-annual component of monthly temperature anomaly along 11°N (2004)

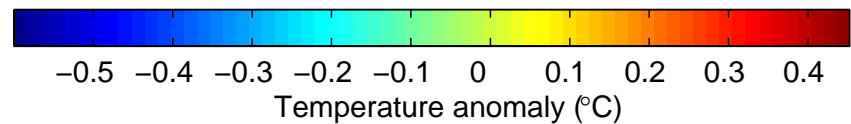
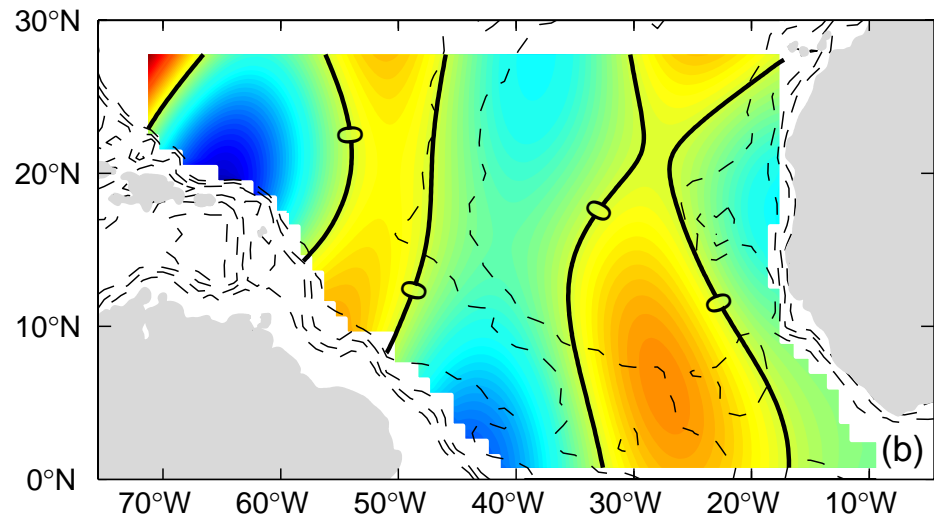
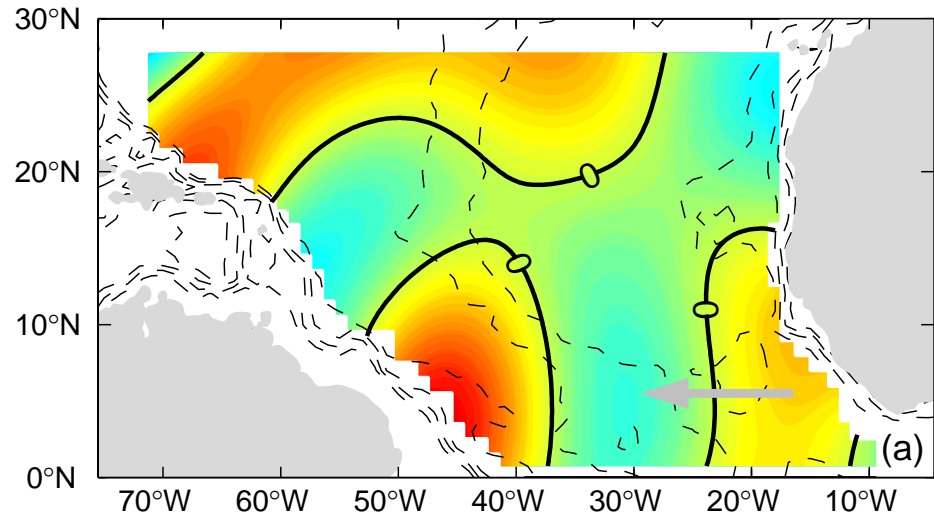
- (a) 6/4
- (b) 7/4
- (c) 8/4
- (d) 9/4



Semi-annual temperature anomaly at 550m depth (2004)

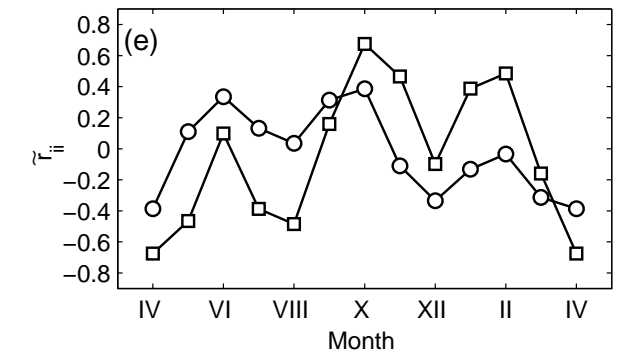
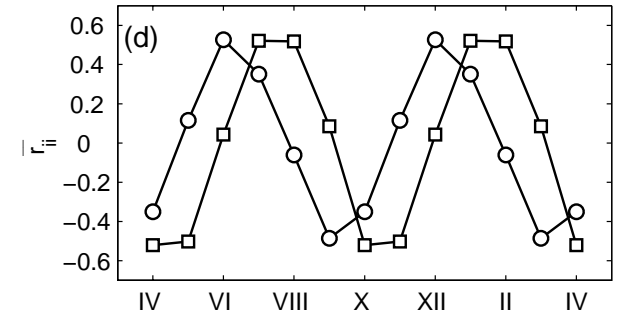
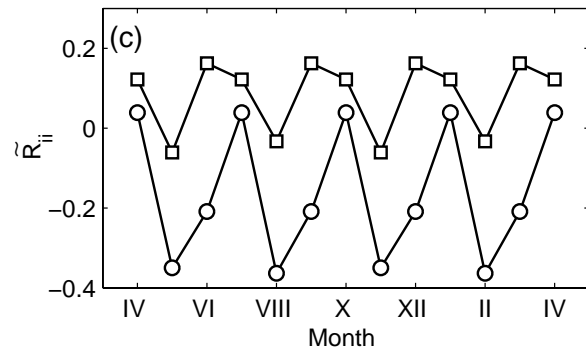
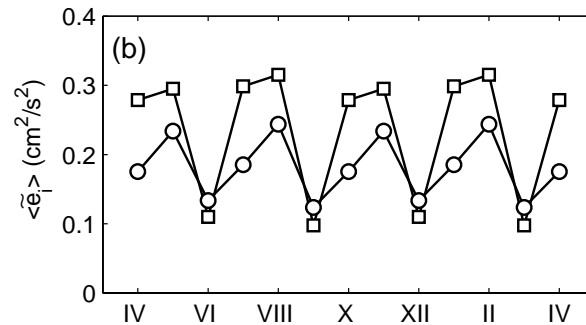
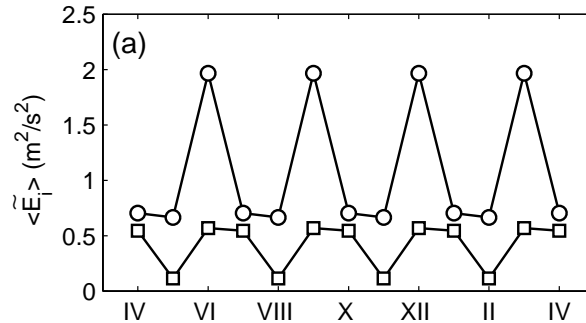
(a) 5/15

(b) 6/29



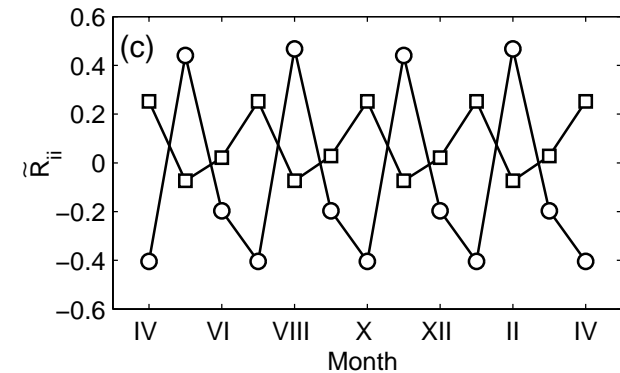
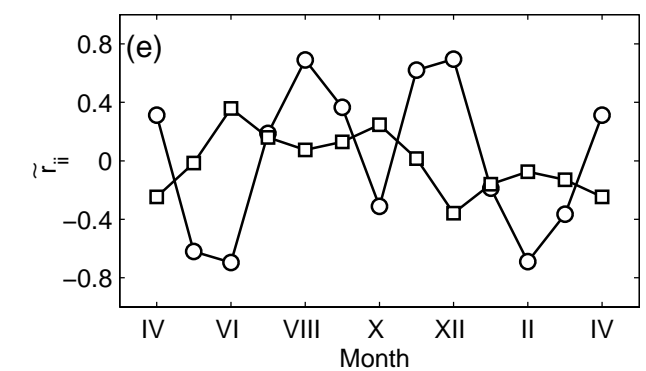
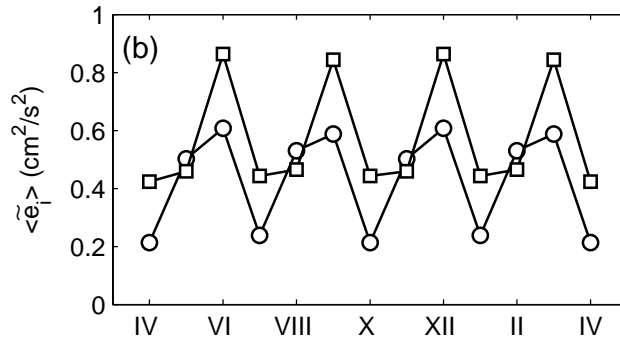
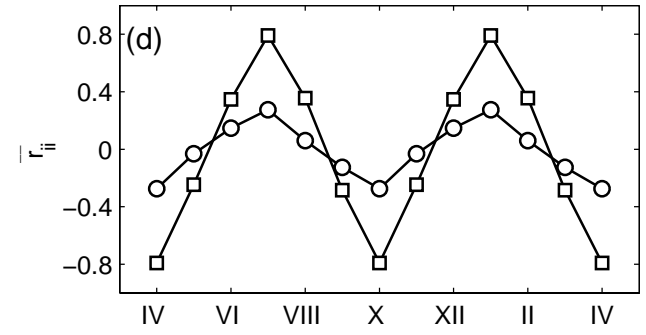
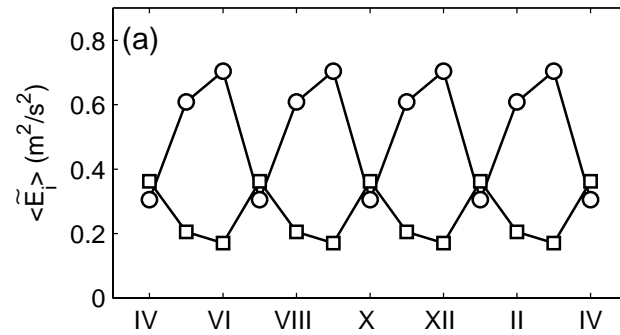
Semiannual Component in the Western Sub-Basin

- (a) wind KE
- (b) current KE
- (c) corr wind stress and currents
- (d) corr between semi-annual currents and mean wind
- (e) corr between semiannual currents and annual wind stress.



Semiannual Component in the Eastern Sub-Basin

- (a) wind KE
- (b) current KE
- (c) corr wind stress and currents
- (d) corr between semi-annual currents and mean wind
- (e) corr between semiannual currents and annual wind stress



Conclusions

- (1) OSD has capability to process ARGO data
- (2) The annual and semi-annual unstable standing Rossby waves are detected in both the western and eastern sub-basins.
- (3) The wind-driven Ekman pumping seems to be responsible for the standing wave generation in both the sub-basins.